JOURNAL OF SOLID STATE CHEMISTRY 75, 251–262 (1988)

Proton Motions in Battery Lead Dioxides

J. R. GAVARRI, P. GARNIER, AND P. BOHER,

Laboratoire CPS, U.A. au CNRS No. 453, Ecole Centrale des Arts et Manufactures, 92295 Châtenay-Malabry Cedex, France

A. J. DIANOUX

I.L.L. Av. des Martyrs 156 X, 38042 Grenoble Cedex, France

AND G. CHEDEVILLE AND B. JACQ

C.E.Ac. 18 quai de Clichy B.P. 306, 92111 Clichy Cedex, France

Received October 20, 1987; in revised form February 9, 1988

Proton motions in α- and β-PbO_2 varieties have been studied using neutron quasielastic scattering in the temperature range 77–300 K. Four varieties of PbO_2 have been characterized: α and β electrochemical PbO_2 and two samples obtained from a battery after two types of cycling. Chemically prepared samples were used to compare quasielastic scattering signals. In electrochemical PbO_2, two types of motions of protons are clearly evidenced: (i) a rotation-like local motion (FWHM = 280 μeV, R = 1.1 Å) which disappears at low temperature or after heating and (ii) a translational motion ($D_t \sim 3 \times 10^{-6}$ cm^2/sec or, using a jump model, $\tau_J = 5 \times 10^{-12}$ sec, $d_J \sim 1.5$ Å). In all samples, a systematic contribution of host lattice is observed in the elastic signals: it might be linked with disordered clusters due to the method of preparation and the presence of protons; two types of elastic contribution can be defined, one connected with some correlations of static distortions.

I. Introduction

Chemically prepared α- and β-PbO_2 are reputed to be electrochemically inactive forms. Active forms have to be prepared by electrochemical process directly on the positive plate of lead batteries.

The reasons for the influence of preparation conditions on the electrochemical properties are not well known at present. In addition, recent results seem to indicate that chemical samples should be electrically active (*1*, *2*).

The exact origin of the battery failure, i.e., the loss of capacity due to cycling, is also unknown. In previous works (*3*), we have established that mechanical factors and chemical and structural changes can play an important role in battery lifetime, the first factors depending probably on the second ones.

An inactive form of PbO_2 could be formed during cycling (*4*); the hypothesis of an electrochemically active amorphous PbO_2 form was emphasized. It could be recrystallized during cycling and transformed

0022-4596/88 $3.00

into an inactive variety similar to the chemical one.

The origin of the electrochemical activity was also linked with the presence of H species (*5*). NMR studies have shown the existence of at least two configurations for protons in electrochemically active PbO_2 and only one configuration for inactive form and chemically prepared PbO_2 (*5*). NMR as well as inelastic (*6*) and neutron quasielastic scattering (NQES) studies (*3*) show that protons are not incorporated in the structure as pure or loosely bound water in pockets.

For β-PbO_2, the chemical analysis of Pb^{4+} content by iodometric titration and of total Pb (Pb^{4+} + Pb^{2+}) by thermogravimetry shows that there is a correlation between H content, measured by neutron transmission, and the difference between the total Pb and Pb^{4+} contents (*7*).

Furthermore, a neutron diffraction study (*6*) has shown that there is no evidence for Pb or O vacancies. In addition, such defects are not necessary for explaining the well-known electrical conductivity of PbO_2. As a consequence, it is generally admitted that the chemical formula is (*3, 6*)

$$Pb^{4+}_{1-x/2}Pb^{2+}_{x/2}O^{2-}_{2-x}(OH^-)_x$$
$$\text{or} \quad Pb^{4+}_{1-x/2}Pb^{2+}_{x/2}O^{2-}_2H^+_x.$$

Both of these formulas can be associated with two extreme chemical states for hydrogen, or equivalently with two types of motions (local, OH^-; jumps, H^+). Our previous studies (*3*) using NQES techniques suggested the existence of at least two types of motions, one of them being a rotation-like one.

II. Structural Background

The α and β phases, respectively orthorhombic and tetragonal, have been extensively described (see (*1, 3, 6*)); both of these phases are characterized by a proton content depending on the chemical or electrochemical preparations. However, protons were never localized. The α and β phases can be differentiated principally from octahedra packings: the orthorhombic and tetragonal lattices of α and β phases are due to different edge sharing of PbO_6 octahedra. As a consequence, the shortest Pb–O and Pb–Pb distances along the two types of PbO_6 chains, in α or β phases, are not aligned in the same directions in each α or β cell. These features are important to understand any structural perturbation due to structural defects. The α phase crystallizes in the orthorhombic system with space group *Pbcm* and $Z = 4$ chemical units.

The β phase crystallizes in the tetragonal system ($P4_2/mnm$ with $Z = 2$: rutile structure). Cell parameters and crystallographic data are given in Table I. The β structure is shown in Fig. 1. It consists of columns of edge-sharing PbO_6 octahedra. These columns are parallel to the *c* axis and form sequences of corner-sharing octahedra along the ⟨110⟩ directions. The two apex Pb–O distances are slightly shorter than the four equatorial ones. The *a* and *c* cell parameters have been found to depend on preparation and cycling. The *a* parameter is greater for fresh battery picked-up samples

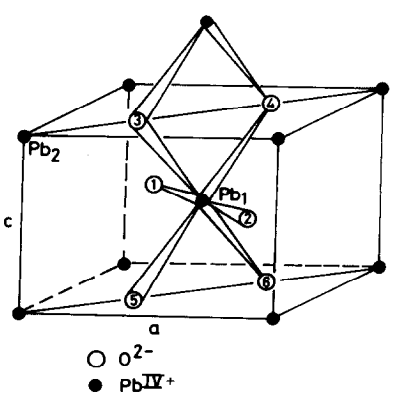

FIG. 1. Structure of the tetragonal PbO_2 β phase.

TABLE I

CRYSTALLOGRAPHIC DATA OF THE β-PbO_2 PHASE

Ref.	Sample and techniques	n (Pb)	a (Å)	c (Å)	x (O)	d (O_3–O_4)
(3)	X ; C		4.965	3.387		
(3)	X ; E		4.951	3.381		
(6)	N ; C	0.986(4)	4.9554(1)	3.3861(1)	0.3068(1)	2.708(1)
(6)	N ; F	0.954(8)	4.9621(2)	3.3856(2)	0.3052(3)	2.734(3)
(1)	N ; C	0.986(10)	4.9556(1)	3.3867(1)	0.3066(2)	
(1)	N ; F	0.950(16)	4.9642(4)	3.3867(3)	0.3054(5)	
(8)	N ; F*	0.967(10)	4.9637(2)	3.3868(1)	0.3063(3)	2.7233(12)
(8)	N ; F**	0.978(10)	4.9658(2)	3.3892(1)	0.3060(3)	2.7243(12)

Note. * Before heating; ** after heating at 260°C, then cooling (20°C). $P4_2/mnm$, $Z = 2$; X, X-ray diffraction; N, neutron diffraction; C, chemical sample; E, electrochemical sample; F, fresh battery sample.

than for chemically prepared samples (*1, 6*). Santoro *et al.* (*6*) have shown that the a parameter decreases when the capacity decreases; it should be larger in active forms than in inactive or chemically prepared β-PbO_2. The c parameter is found to be unchanged.

Another feature is the following: the departure of H species (as H_2O molecules), by heating at 260°C at normal pressure, causes a systematic increasing of both a and c parameters with a strong variation for the latter. This result was first obtained from X-ray diffraction on chemical and electrochemical samples (*3*) and recently confirmed by neutron diffraction on a fresh battery picked-up sample (*8*). The principal conclusions of this last study can be summarized as follows:

—Before heating, proton species cannot be located on special sites: a Fourier map was attempted at the end of structural refinements without success.

—After heating at 260°C and cooling, the departure of protons is connected with the increase of both a and c parameters (Table I): the Pb–O distances remain unchanged while some of the O–O distances are modified.

—Only a small Pb deficiency might be defined before and after heating from the site occupation factors; however, the Debye–Waller factors are large (B = 1.3 to 1.6 Å^2) and the diffraction profiles present small distortions.

—After heating, a continuous and constant decrease of the background is observed all along the diffraction range.

Such results can be understood only if charged proton species are present in the lattice: for example, H^+ located between two oxygen of an octahedron [PbO_6] should induce a contraction of O–O distance. On the contrary, the presence of neutral water structurally intercalated would have induced an isotropic volume expansion; as a consequence the departure of such neutral molecules after heating would have been associated with a decrease of cell volume, which is not the case.

Considering these results and by analogy with SnO_2 and TiO_2, we are able to postulate the existence of OH^- species substituting for O^{2-}. As we reduce Pb^{4+} into Pb^{2+} we suppose that two OH^- are located near a Pb^{2+} ion; such OH^- species should be lying along the ⟨110⟩ direction on the common edge of two octahedra (*3*). As a result

some O–H . . . O bonds in the ⟨110⟩ direction should be formed and randomly distributed in the structure. Obviously, the other edges of PbO_6 octahedra might be visited by the proton which can move more or less rapidly around one oxygen.

The elimination of protons as H_2O molecules (*8, 10, 12*) by heating corresponds to the reaction

$$Pb^{4+}_{1-x/2}Pb^{2+}_{x/2}O^{2-}_{2-x}(OH^-)_x \rightarrow Pb^{4+}_{1-x}Pb^{2+}_{x}O^{2-}_{2-x/2}\square_{x/2} + \frac{x}{2}\overrightarrow{H_2O} - xe^-.$$

Thus, it causes the formation of some vacancies on oxygen sites and consequently increases the Pb^{2+} content. This result has two outcomes:

—The Pb^{2+}–O bonds are longer (2.21–2.48 Å) than the Pb^{4+}–O bonds (2.13–2.17 Å); therefore, the elimination of protons induces a global increase of the cell volume (*3*).

—The vacancies on oxygen sites induce direct contact between Pb^{2+} ions in a direction parallel to the *c* axis (3.38 Å). This extra repulsion makes the cell distortion more important in the *c* direction than in the *a* and *b* directions after heating (*3*).

Considering all the structural evidence we have postulated the existence of several motions:

(1) a jump between the two oxygens (for example O_3–O_4) of a common edge; if we considered $d_{OH} \sim 1.1$ Å the jump distance should be ~0.5 Å;

(2) a rotation-like motion, on a sphere of radius R_O (~0.9–1.2 Å), around an oxygen atom;

(3) a rotation-like motion on a sphere of radius R_{Pb} (~1.5–1.7 Å) if H is supposed to rotate around a Pb atom, all the octahedron edges being visited.

III. Experiments

III.1. Origin and Analysis of Samples

Six samples have been investigated and characterized by iodometric titration to determine the Pb^{4+} content and the quantities of H species present in the structure (H contents have been confirmed by neutron studies and thermogravimetric analysis (*8, 10*)):

—Chemical α-PbO_2 (referred to as C_α) is prepared by oxidizing lead acetate in solution with an excess of ammonium persulfate in the presence of ammonium acetate and ammonia (*7*). Its composition corresponds to $x = 0.14$.

—Chemical β-PbO_2 (C_β) is a commercial product, "Fluka for analysis," and corresponds to $x = 0.05$.

—Electrochemical α-PbO_2 (E_α) is prepared by the method described by Nguyen Cong *et al.* (*9*); $x = 0.10$.

—Electrochemical β-PbO_2 (E_β) is prepared by electrolysis of a 0.5 *M* solution of $Pb(NO_3)_2$ in HNO_3 and is characterized by $x = 0.14$.

—Two samples are picked up from the positive plate of lead batteries after 50 cycles (B_{50}) and 860 cycles (B_{860}). B_{50} corresponds to the maximal capacity of the battery and B_{860} to its failure[1] (*10*). The inhomogeneity (sulfate residue) makes the analysis imprecise for these samples.

III.2. Quasielastic Neutron Scattering

QENS experiments have been performed on the IN5 spectrometer of the I.L.L. All experiments on electrochemical samples have been performed using the same experimental procedure (beam incidence, Al container, thermal treatment . . .). All samples have been heated previously at 150°C for 24 hr to eliminate adsorbed water.

[1] Samples given by C.E.Ac.

Samples were stored and transported in the same container under vacuum.

A cryostat has been used in order to observe the evolution of the QES signal when freezing proton motions in the range 77–300 K.

Two incident wavelengths were chosen ($\lambda = 5$ and 10 Å); they allow us to separate two possible types of motions because of two resolutions: $\Delta E \sim 18$ μeV for $\lambda = 10$ Å and $\Delta E \sim 120$ μeV for $\lambda = 5$ Å. In addition for IN5 the elastic scattering profile is triangular so that small Lorentzian signals due to QES are easily detectable.

IV. Results and Discussions

IV.1. Contribution of Host Lattice

An important feature is observed: the host lattice is responsible for a supplementary signal which is attributed to structural disorder, probably static distortions due to chemical preparation and presence of protons.

This component has been first evaluated by studying two samples (C_α and C_β), the compositions of which are well known and quasielastic scattering experiments previously described (*3*).

The host lattice component has been obtained by extrapolating at $x = 0$ the various intensity functions $I(Q)$ for several Q values. The ESFIT5 program permits the separation of the elastic (I_E) and quasielastic (I_{QE}) components of signals $I(Q)$. The elastic fraction (EISF) is expressed by

$$\rho = \frac{I_E}{I_{QE} + I_E} = \frac{I_{HL} + I(H)}{I_{QE} + I_{HL} + I(H)} = b + \frac{I(H)}{I_{Total}},$$

where $b = I_{HL}/I_{total}$ and I_{HL} is the host lattice elastic scattering (including fixed protons).

If the elastic incoherent structure factor due to mobile protons is $A(Q) = I(H)/(I_{QE} + I(H))$ and $b(Q)$ is the elastic contribution of the disordered host lattice, one can write:

$$\rho = b + (1 - b) \cdot A^{obs}(Q). \qquad (1)$$

For C_α and C_β it has been possible to define a quasiconstant b value in the whole range $0.9 < Q < 1.9$ Å^{-1} out of Bragg peaks,

$$b = 155/(155 + 6.74\,x), \qquad (2)$$

where x is the concentration of H expressed in percentage. For $x = 10$, $b \sim 0.70$; this means that only 30% of signal is due to protons.

The two samples have been chemically prepared but we have supposed in this evaluation that b is not too dependent on the type of structure (α or β) nor on the chemical or electrochemical preparation procedure. Thus, the b value obtained from the expression (2) is only an approximate value and is used as a first suitable value for refinement; it will be refined and confirmed later. We have found $b \sim 0.62$ for E_β ($x = 14\%$) and $b \sim 0.70$ for E_α ($x = 10\%$). From relation (1) one obtains $A^{obs}(Q)$ which is related to the geometry of proton motions. Correlatively if the geometry of the motion is known it is possible to calculate $A(Q)$ then to refine b which is characteristic of elastic scattering from host lattice.

IV.2. Results at $\lambda = 5$ Å

The jump model on two sites (*13*), with a jump distance $d_J \sim 0.5$–0.6 Å, could not fit the data. A second model has been found to be representative of experimental data. It is the rotational diffusion on the surface of a sphere of radius R (*14*).

This model depends on a parameter D_R. The effective mean HWHM is known to be close $2D_R$; the FWHM being $4D_R$ as a first approach.

The EISF is given by

$$A(Q) = \left(\frac{\sin QR}{QR}\right)^2.$$

Such a model has allowed us to fit the signals obtained for $\lambda = 5$ Å; it was fitted first for the E_β sample.

In order to calculate the radius of the rotation, the elastic contribution $b(Q)$ had to be refined. A first calculation was possible using the Debye–Waller (DW) factors obtained from intensities at two temperatures: 150 and 310 K. The following expression is used:

$$I = I_0^{-Q^2\langle u\rangle^2} = I^0_{HL}e^{-Q^2\langle u^2_{HL}\rangle} + I^0_H e^{-Q^2\langle u^2_H\rangle},$$

where $I_0 = I^0_{HL} + I^0_H$, $b = I^0_{HL}/I_0$ and where $\langle u^2\rangle$ is the mean square amplitude of vibration (MSAV). One has the relation used as an approximation,

$$\langle \Delta u^2\rangle^{obs} = \langle u^2\rangle_{310} - \langle u^2\rangle_{150} = \Delta u^2_{HL} b + (1 - b)\Delta u^2_H,$$

where Δu^2_{HL} and Δu^2_H are the variation of MSAV of host lattice (Pb and O) and protons.

Observed values of $\langle \Delta u^2\rangle$ for E_β are given in Table II as a function of Q. For Bragg peaks the variation of intensities are principally due to host lattice. Using the Bragg peaks we obtained $\Delta u^2_{HL} = 0.010$ Å^2 (for $Q = 1.81$ Å^{-1}).

The observed $\langle \Delta u^2\rangle$ values allow us to find a mean Δu^2_H value and to evaluate the effective b values for each Q. Using these refined b values it is then possible to define a unique $\langle \Delta u^2_H\rangle$ value: $\langle \Delta u^2_H\rangle = 0.15$ Å^2.

The $b(Q)$ effective value being determined, the fit is operated in fixing R at various values lying in the range 0.8–2 Å and refining the D_R parameter from the rotational diffusion model of Sears. The model is considered to be well fitted when D_R values, calculated for each Q values, are quasiconstant; this criterion was satisfied for $R = 1.1 \pm 0.1$ Å. Under these conditions the mean D_R value is found equal to 70 μeV which corresponds to FWHM = 280 μeV.

Figure 2 represents some of the fits. Table III gives the results of last calculations obtained for the E_β sample. The elastic fraction obtained from a model independent fit is recalled; the observed and calculated val-

TABLE II

EVOLUTION OF $\langle \Delta u^2\rangle$ IN THE RANGE 310–150 K AS A FUNCTION OF Q (Å^{-1}) AND CORRESPONDING REFINED b VALUES FOR E_β SAMPLE

Q	$\langle \Delta u^2\rangle$ (310–150 K)	b (Q)
0.34	0.47	~0.8
0.53	0.15	0.002
0.74	0.076	0.36
0.94	0.076	0.43
1.134	0.070	0.61
1.319	0.071	0.67
1.494	0.050	0.76
1.66	0.049	0.78
1.81	0.017	0.987
1.93	0.026	0.857
2.1	0.034	0.823

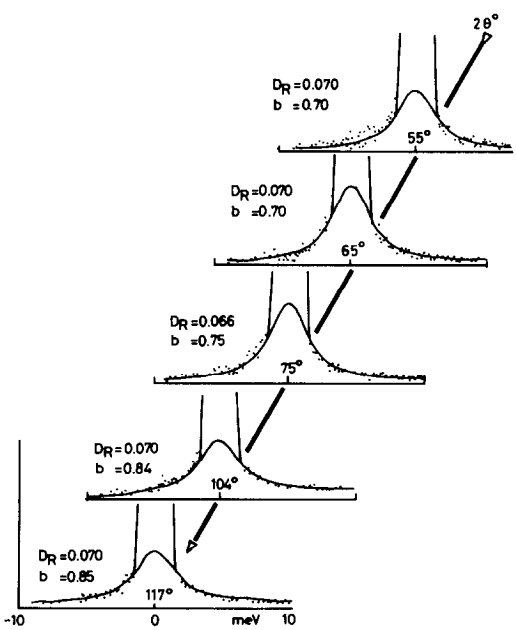

FIG. 2. Characteristic fits for $\lambda = 5$ Å. D_R is constant and b is refined.

TABLE III

QUASIELASTIC DATA AT $\lambda = 5$ Å

Q (Å^{-1})	ρ_{fit}	A_{obs}	A_{calc}
0.53	0.970	0.970	0.89
0.74	0.874	0.800	0.80
0.94	0.820	0.680	0.69
1.134	0.838	0.584	0.58
1.319	0.823	0.660	0.47
1.494	0.834	0.300	0.368
1.66	0.846	0.309	0.280
1.81	0.990[a]	0.230	0.210
1.93	0.885	0.196	0.156
2.10	0.850	0.152	0.102

Note. Fits for E_β sample at 30°C ($D_R = 70 \pm 20\ \mu$eV, $R = 1.1 \pm 0.2$ Å, $A_{calc} = (\sin QR/QR)^2$).

[a] Bragg peak.

ues A^{obs} and A^{calc} are compared. The program then allows us to refine the individual $b(Q)$ values for R and D_R fixed. These values are found to be close to the initial ones.

In Table IV we have gathered the refined elastic scattering component $b(Q)$ for the four samples E_β, E_α, B_{50}, and B_{860} at 310 K and for E_β at 150 K. Even measurements including Bragg peaks have been treated. We may note that b for $Q > 1$ Å^{-1} (out of Bragg peaks) is greater for E_α than for E_β and for B_{860} than for B_{50}. This means that the contribution due to protons is, relative to the host lattice one, less important for E_α, which has less proton (10%), than for E_β (14%) and less important for B_{860} (end of life) than for B_{50} (fresh battery).

IV.3. Results at $\lambda = 10$ Å

We have taken into account the previous results obtained at $\lambda = 5$ Å. At $\lambda = 10$ Å the elastic contribution of the total signal is such that:

$$b^*(Q) = \frac{I'_{HL}}{I_{Total}(\lambda = 10\ \text{Å})} = \frac{I_{HL} - I_H^{(2)}}{I_{HL} + I_H^{(2)} + I_H^{(1)}} = \frac{b}{\rho(5\ \text{Å})} - \frac{I_H^{(2)}}{\rho(5\ \text{Å})}.$$

In this expression $I_H^{(2)}$ is the term describing the second proton motion, while $I_H^{(1)}$ is that obtained at $\lambda = 5$ Å (rotation); at $\lambda = 10$ Å the I_{QE} component due to rotation has vanished in the background. The effective host lattice contribution is I'_{HL}. As a first approach the term $I_H^{(2)}/\rho$ was neglected.

Using the $b(Q)$ values at $\lambda = 5$ Å it has been possible to evaluate the b^* elastic term (for $\lambda = 10$ Å) in the range 0–1 Å^{-1}; under that condition a small quasielastic contribution has been detected at 310 K. This contribution disappears at 150 K.

In the range $Q = 0.15$–0.4 Å^{-1} the elastic contribution is strong (Figs. 3 and 4). However, between $Q = 0.5$ and $Q = 1.2$ Å^{-1} a weak increasing quasielastic signal is observed in each sample. Table V gathers the principal results obtained at $\lambda = 10$ Å. The $I(Q)$ values are represented in Figs. 3 and 4. Figure 5 shows the observed HWHM for each sample. At $Q = 0.7$ Å^{-1}, HWHM $\sim 10 \pm 2\ \mu$eV, and at $Q = 1.2$ Å^{-1}, HWHM $\sim 25 \pm 5\ \mu$eV.

The systematic evolution should be as-

TABLE IV

REFINED ELASTIC COMPONENTS b AT $\lambda = 5$ Å FOR FOUR SAMPLES AS A FUNCTION OF Q

	E_β				
Q (Å^{-1})	310 K	150 K	E_α	B_{50}	B_{860}
0.32	0.72	0.93	0.85	0.82	0.92
0.36	0.09	0.001	0.30	0.42	0.57
0.53	0.002	0.005	0.00	0.19	0.006
0.74	0.36	0.86	0.705	0.55	0.79
0.94[a]	0.43	1.00	0.93	0.85	0.92
1.134	0.61	0.51	0.71	0.69	0.80
1.319	0.67	0.54	0.72	0.72	0.81
1.494	0.76	0.59	0.74	0.75	0.82
1.66	0.78	0.71	0.92	0.82	0.85
1.81	0.99	1.00	0.87	0.98	0.98
1.93	0.86	0.93	0.87	0.82	0.87
2.10	0.82	0.16	0.87	0.83	0.89
⟨b⟩[b]	0.68(8)	0.54(4)	0.72(2)	0.72(3)	0.81(1)

Note. The starting values are $b_0 = 0.62$ for the β variety and $b_0 = 0.695$ for the α one. The B_{50} and B_{860} samples are principally of the β variety.

[a] Close to $Q = 0.94$ Å^{-1} an anomaly is observed in the case of E_α, B_{50}, B_{860} samples.

[b] Averaged b values obtained in the range $1 < Q < 1.5$ Å^{-1}.

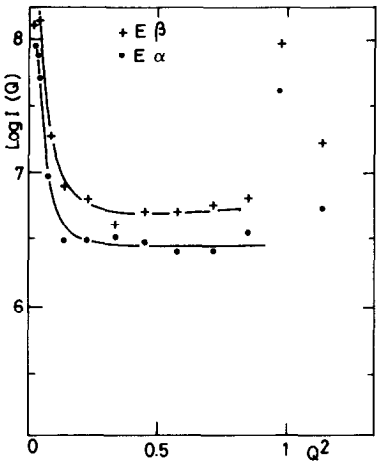

FIG. 3. Intensities observed at $\lambda = 10$ Å for E_α and E_β samples as a function of Q^2.

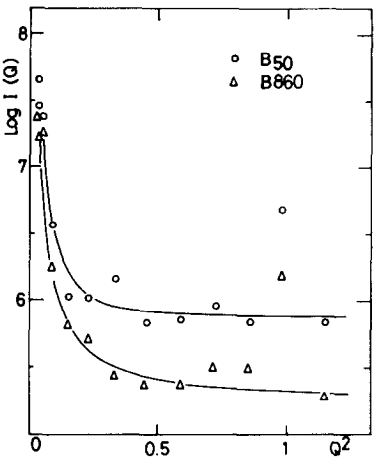

FIG. 4. Intensities observed at $\lambda = 10$ Å for B_{50} and B_{860} samples as a function of Q^2.

cribed to some translational motion because of the apparent Q^2 variation of HWHM. Two types of motions can be postulated.

(a) a continuous translation through the lattice with HWHM $= D_t Q^2$ so that

$$D_t \sim (3 \pm 1) \times 10^{-6} \text{ cm}^2 \text{ sec}^{-1};$$

(b) a jump model (the Chudley–Elliot model) with jump distances d_J corresponding to cubic configuration and with residence time τ_J.

$$S(Q, \omega) = \frac{1}{\pi} \frac{f(Q)}{f^2(Q) + \omega^2}$$

$$\text{FWHM} = 2f(Q) = \frac{1}{\tau_J}\left[1 - \frac{\sin Qd_J}{Qd_J}\right].$$

Considering the same motion for each sample one obtains:

$$\tau_J = (0.5 \pm 0.3) \times 10^{-11} \text{ sec}$$

$$d_J = 1.5 \pm 0.5 \text{ Å}.$$

TABLE V

QUASIELASTIC SCATTERING AT $\lambda = 10$ Å (FIT OF ONE LORENTZIAN): ELASTIC CONTRIBUTION OF HOST LATTICE (b) AND HWHM IN μev

Q (Å^{-1})	$\langle b^a(Q)\rangle$	HWHM (μeV)
0.15	0.95	<1.
0.27	0.70	1.
0.48	0.20	2. ± 1.
0.68	0.75	6. ± 3.
0.95	0.95	20. ± 10.
1.07	0.85	20. ± 15.

[a] b values are the average values for the four samples.

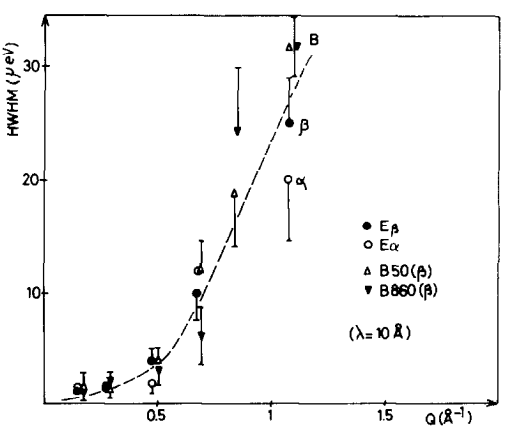

FIG. 5. HWHM as a function of Q for $\lambda = 10$ Å.

In Fig. 5 a small tendency for larger diffusion rate is observed in the case of cycled samples but due to the incertainty it is not possible to draw conclusions about it. Using the Z_J and d_J values it is possible to calculate a D_t coefficient (cubic configuration):

$$D_t = \frac{d_J^2}{6\tau_J} = 7.2 \times 10^{-6} \text{ cm}^2 \text{ sec}^{-1}.$$

With a d_J limit value of 1 Å one obtains $D_t \sim 3.2 \times 10^{-6}$ cm^2 sec^{-1} which is in the range of D_t values for continuous translational motions.

The mean d_J value can be compared with expected jump distances on octahedron edges. Along the c axis the jump (O_3–O_5) can be evaluated using

$$c = 2d_{OH} + d_J = 3.38 \text{ Å};$$

with $d_{OH} = 1.1$ Å (rotation radius) we obtain $d_J \sim 1.18$ Å.

From one edge to another, a jump distance in the range 0.9–1.5 Å can be expected. As a consequence successive jumps all along octahedron edges and along the c direction can be expected; this can be described by mean $\langle d_J \rangle$ values of about 1 to 1.5 Å.

IV.4. Proton Population and Host Lattice Contribution

The quasielastic signals at $\lambda = 5$ and 10 Å have been treated independently. At 5 Å, in the range $1 < Q < 2$ Å^{-1} out of Bragg peaks, the b value is slowly increasing: at $Q = 1.3$ Å^{-1}, $b \sim 0.65$. At $\lambda = 10$ Å the b^* value is calculated after postulating $b^* = b/\rho$; for $Q = 0.74$ Å^{-1}, $b^* \sim 0.5$, and for $Q = 1.1$ Å^{-1}, $b^* \sim 0.73$.

The b and b^* values can be compared to the following expressions:

$$b(Q) \simeq \frac{K\sigma_{PbO_2}(1 - D_S) + \sigma_H^{inc.} xP_2DW}{K\sigma_{PbO_2}(1 - D_S) + \sigma_H^{inc.} xP_2DW + \sigma_H^{inc.} xP_1DW}$$

$$b^*(Q) \simeq \frac{K\sigma_{PbO_2}(1 - D_S) + \sigma_H^{inc.} xP_2DW}{K\sigma_{PbO_2}(1 - D_S) + \sigma_H^{inc.} xP_2DW + \sigma_H^{inc.} xP_1DWA(Q)},$$

where $\sigma_H^{inc.} = 80$, $x \sim 0.14$ (atomic concentration in the well known β phase E_β), K is the proportion of host lattice involved in distortions, $\sigma_{PbO} = 19.3$ is the total (incoherent + coherent) scattering contribution of one formula PbO_2, D_S is the static distortion term considered as the approximate function $D_S = e^{-Q^2\langle u_{st}^2 \rangle}$, $\langle u_{st}^2 \rangle$ represents the disordered distortions due to defects, DW is the Debye–Waller term associated with proton vibrations ($e^{-Q^2\langle u_{th}^2 \rangle}$, where $\langle u_{th}^2 \rangle$ is taken to be equal to 0.30 Å^2), P_1 and P_2 are the populations of protons involved in independent motions (rotations and translations, respectively).

In these expressions, correlated motions have not been considered because of poor statistics and large uncertainties concerning all models; thus, $P_1 + P_2 = 1$.

The principal difficulty was to evaluate the contribution of elastic diffuse scattering (EDS); apparently the first undulation of the $b(Q)$ function suggests the existence of some correlations in distortions. However, we tried to evaluate the D_S term by fitting a crude function to the experimental points $b(Q)$ at $Q \sim 0.5$ and 1.3 Å^{-1}; we have obtained $u_{st}^2 \sim 0.5 \pm 0.3$ Å^2.

Then using the values of b and b^* respectively at $Q = 1.3$ Å^{-1} and at $Q = 0.74$ or 1.1 Å^{-1} it was possible to obtain the order of magnitude for P_1, P_2, and K:

$K = 0.5 \pm 0.3$, $P_1 = 0.65 \pm 0.2$,
$P_2 = 0.35 \pm 0.2$.

In other terms the host lattice might deliver an incoherent signal of one-half of the total scattering; among protons in motions two-thirds should be engaged in rotations (P_1) and about one-third in continuous translations (P_2).

IV.5. Small Angle Scattering and Proton Concentration

Small angle scattering has been observed for all the samples. An example is given in Figs. 3 and 4 in the case of $\lambda = 10$ Å for the four studied samples. First, in Fig. 3 we note that the intensity is more important for E_β for which proton content is greater ($x = 0.14$ instead of $x = 0.10$ for E_α). A difference is also noted between B_{50} and B_{860}. A direct comparison is difficult between the two sets of samples (battery samples and electrochemical samples) but it is probable that B_{860} contains less protons than B_{50}. Such a hypothesis has already been emphasized.

These observations have to be correlated with the relative contribution of the host lattice to the incoherent signal: $b(\beta) < b(\alpha)$ for $x(\beta) > x(\alpha)$ and $b(B_{50}) < b(B_{860})$.

The intensity at small angle is probably related to the presence of clusters as suggested previously (*3*). The density of clusters seems directly connected with the proton concentration of the samples.

In the picked-up samples, B_{50} and B_{860}, the evolution of signals with cycling, argue in favor of cluster density decrease, i.e., proton elimination during cycling.

Figure 6a represents the general variations observed for $b(Q)$; a systematic minimum is observed at $Q = 0.5$ Å^{-1} for each sample. An undulation of $b(Q)$ might be defined at $Q > 1$ Å^{-1}. In Figs. 6b and 6c, the small angle scattering and the EDS term due to coherent scattering from distortions are represented (rough estimates). The superposition of both features might explain our present observations. It is important to note that the maximum at $Q \sim 0.95$ Å^{-1} has been confirmed in experiments at $\lambda = 10$ Å (Figs. 3 and 4).

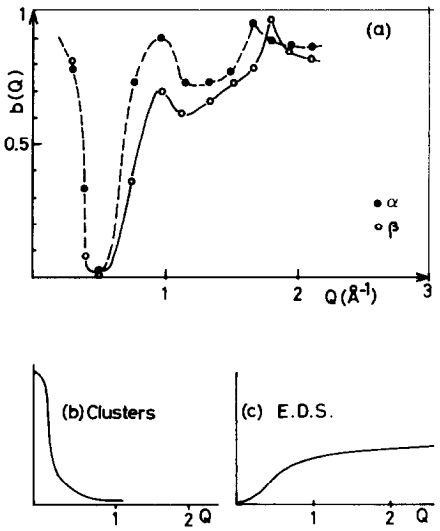

FIG. 6. Elastic contribution of host lattice ($\lambda = 5$ Å) as a function of Q.

V. Conclusion

V.1. Types of Motions

Table VI summarizes the principal results obtained in this study. We have established the existence of at least two types of proton motions in agreement with the two chemical formulas mentioned under the Introduction:

(1) a local motion similar to an OH^- hindered rotation (radius, 1.1 Å);

(2) a long-range translation motion which can be either continuous ($D_t \sim 3 \times 10^{-6}$ cm^2 sec^{-1}) or not (residence time, $\tau_J = 0.5 \times 10^{-11}$ sec, jump distance ~ 1.5 Å).

If two types of protons are postulated the population of protons in rotation is about 65% while that of protons in long-range translation should be about 35%.

TABLE VI

SUMMARY OF PRINCIPAL RESULTS AT $\lambda = 5$ Å AND $\lambda = 10$ Å FOR THE ROTATION MODEL (R), THE CONTINUOUS TRANSLATION MODEL (D_t), AND THE CHUDLEY–ELLIOT MODEL (d_J, τ_J, D_T)

Characteristics	$\lambda = 5$ Å	$\lambda = 10$ Å
FWHM (μeV)	280.	Q dependent
R (Å)	1.1 ± .2	
D_t (cm^2 sec^{-1})		3. ± 1. 10^{-6}
d_J (Å)		1.5 ± 0.5
τ_J (sec)		0.5 10^{-11}
D_T (cm^2 sec^{-1})		7.2 10^{-6}
P_t (%)	65 ± 20	35 ± 20
K (%)	50 ± 30	50 ± 30

Note. P_t and K are, respectively, the contribution of each movement and of the host lattice (see text). The given data are the average value obtained for all the samples.

The translational motion with $D_t = 3 \times 10^{-6}$ cm^2 sec^{-1} can be directly compared with the value recently found by Münzberg and Pohl (*11*) for the chemical diffusion coefficient of hydrogen in PbO_2 obtained from the electrochemical method at various pHs and concentrations of Pb^{2+}:

$$\tilde{D}_H \sim 0.4 \text{ to } 4.9 \times 10^{-7} \text{ cm}^2 \text{ sec}^{-1}.$$

Such a coefficient is linked to the D_t coefficient by the relation

$$\tilde{D}_H = D_t \frac{d \ln a}{d \ln c},$$

where a and c are, respectively, the activity of protons and the concentration of Pb^{2+} within the solid, i.e., of proton in the oxide. The order of magnitude of the experimental D_t coefficient can be considered to be in agreement with $\tilde{D}_H$, which is necessarily smaller than D_t.

In addition, it has been observed as an important contribution of the host lattice to the elastic signals: at small Q values, strong elastic components indicate the presence of small clusters. Such clusters are probably domains with smaller specific volume and in which protons are agglomerated. The long-range motion (D_t) might be connected with migration between clusters. Inside cluster zones, protons might be trapped with rotation-like motions.

In electrochemical samples protons should be more dilute than in chemical samples (*3*). The cycling procedure of batteries should be associated with elimination of "free protons" (the long-range diffusion signal was not observed in chemically prepared samples (*3*)); this cycling should induce condensation in larger domains or elimination from the bulk due to diffusion through grain surfaces.

The host lattice is found to be disordered (large b values ~ 50% for the global contribution for both $\lambda = 10$ Å and $\lambda = 5$ Å spectra). This disorder is directly connected with the presence of clusters.

V.2. Clusters and Chemical Reactivity

Let us recall the condensed chemical formula of lead dioxide:

$$Pb^{4+}_{1-x/2}Pb^{2+}_{x/2}O^{2-}_2H^+_x.$$

The presence of clusters is evidenced by the following developed formula (if we first consider that all protons are trapped in the clusters):

$$\left(1 - \frac{x}{2}\right)[Pb^{4+}O^{2-}_2] + \frac{x}{2}[Pb^{2+}(OH^-)_2].$$

Two types of domains appear: the lattice of composition PbO_2 and the clusters of composition $Pb(OH)_2$. The volume ratio of the two types of domains is $(x/2)/(1 - x/2)$. When the lead dioxide is heated the clusters of composition $Pb(OH)_2$ probably first decompose into PbO clusters because of the lower thermal stability of Pb^{2+}–$(OH)^-$ bonds:

$$Pb^{2+}(OH)^-_2 \rightarrow Pb^{2+}O^{2-} + \overrightarrow{H_2O}.$$

This process has been confirmed by mass spectroscopy measurements; the first step

of decomposition is characterized by departure of water molecules (*8, 10*). The influence of protons (trapped in clusters or isolated) on the chemical reactivity, especially on reduction (in monoxide or sulfate), is yet to be postulated (*5, 12*).

So as a first step of decomposition we have the juxtaposition of a matrix of composition PbO_2 and microzones of composition PbO. This juxtaposition is possible because the packing of lead atoms is the same for all lead oxides in the range PbO_2–PbO (except for Pb_2O_3 and Pb_3O_4 (*12*)), the electron lone pairs of Pb^{2+} ions playing the stereochemical role of oxygen atoms.

Thus, the existence of zones of different compositions according to the density of clusters is coherent with our previous model of decomposition (*12*). The intermediary pseudocubic lead oxides PbO_x (x = 1.57 and x = 1.41) may be interpreted thanks to the presence of different zones: for example, $PbO_{1.57}$ could be considered to be the juxtaposition of zones of composition $Pb_{24}O_{40}$ and $Pb_{24}O_{36}$ (*12*).

We have seen that all protons are not trapped in clusters but are involved in translational motions. Such protons are disseminated in the bulk. Both types of protons probably induce displacements of lead atoms (the Pb^{2+} ions), which do not scatter coherently with the host lattice. Therefore the effective diffraction pattern should be due to a more complex average structure corresponding to the mean formula

$$Pb^{4+}_{1-x/2}Pb^{2-}_{x/2}O^{2-}_{2-x}(OH^-)_x,$$

where the index $x/2$ corresponds to virtual vacancies because of the displacements of Pb^{2+} from the theoretical site (Pb^{4+}).

This may explain the apparent Pb vacancies observed in our own neutron diffraction refinements (Table I).

Acknowledgment

The work was performed with financial support from the AFME.

References

1. R. J. Hill, *Mater. Res. Bull.* **17,** 769 (1982).
2. G. Chedeville, personal communication.
3. P. Boher, P. Garnier, and J. R. Gavarri, *J. Solid State Chem.* **52,** 146 (1984).
4. S. M. Caulder and A. C. Simon, *J. Electrochem. Soc.* **121,** 1546 (1974).
5. S. M. Caulder, J. S. Murday, and A. C. Simon, *J. Electrochem. Soc.* **120,** 1515 (1973).
6. A. Santoro, P. D'Antonio, and S. M. Caulder, *J. Electrochem. Soc.* **130,** 7, 1451 (1983).
7. P. T. Moseley, J. L. Hutchison, C. J. Wright, M. A. M. Bourke, R. I. Hill, and V. S. Rainey, *J. Electrochem. Soc.* **130,** 829 (1983).
8. P. Boher, P. Garnier, J. R. Gavarri, P. Gregoire, L. Abello, to be published (1988).
9. H. Nguyen Cong, A. Ejjenne, J. Brenet, and P. Faber, *J. Appl. Electrochem.* **11,** 373 (1981).
10. P. Boher, Thesis, Paris (1984).
11. R. Münzberg and J. P. Pohl, *Z. Phys. Chem.* **146,** 97 (1985).
12. P. Boher, P. Garnier, J. R. Gavarri, and D. Weigel, *J. Solid State Chem.* **55,** 54 (1984).
13. A. J. Dianoux, F. Volino, and H. Hervet, *Mol. Phys.* **30,** 1181 (1975).
14. V. F. Sears, *Canad. J. Phys.* **45,** 237 (1967).